Articles

Gold-Nanoparticle-Infiltrated Polystyrene Inverse Opals: A Three-Dimensional Platform for Generating Combined Optical Properties

Yong Tan, Weiping Qian,* Shaohua Ding, and Yi Wang

State Key Laboratory of Bioelectronics, Department of Biological Science and Medical Engineering, Southeast University, Nanjing 210096, People's Republic of China

Received January 26, 2006. Revised Manuscript Received May 20, 2006

Photonic crystals incorporating metal nanoparticles have recently attracted increasing interest because they may open a way to generate novel optical properties. Although they provide an opportunity to manipulate combined optical signals, to date, optical properties of these composite materials have been scarcely investigated. Here, we present the first example of gold-nanoparticle-infiltrated polystyrene (GNIPS) inverse opals, which not only preserve localized surface plasmon resonance (LSPR) properties of gold nanoparticles (GNPs), but also replicate photonic features from templates. By varying the refractive index (RI) and the incident angle, the relative shifts between resonance peaks and diffraction peaks are observed. On the basis of the volatilization kinetics of ethanol within the GNIPS films, we investigate the external interactions of LSPR and photonic band gap (PBG). It is found that the LSPR peak of GNPs in GNIPS is unexpectedly red-shifted with the decrease of effective RI. Additionally, due to the reversible change of the two characteristic peaks, these GNIPS films exhibit an optical "on−off switching" capability, which is useful in monitoring the changes of the microenvironment by the permeation and release of surrounding media.

Introduction

Photonic crystals (PCs)[1] and noble metal nanoparticles (NMNs)[2] have been extensively studied in the past decade because of their attractive properties involving photonic band gap (PBG) and localized surface plasmon resonance (LSPR),[3] respectively. With a few exceptions,[4] PCs and NMNs generally are explored in two separated research areas. Recently, however, growing interests[5−7] in the incorporation of these two kinds of materials have emerged due to the unique optical properties of new composite materials. One of the most important forms among these new materials is NMN-infiltrated composite PCs, which have attracted considerable attention because of their potential applications in photonics, catalysis, and sensing. To date, various types of composite PCs incorporating NMNs have been fabricated, such as metal-coated three-dimensionally ordered macroporous (3DOM) film, metal-dielectric opals, and metal-dielectric inverse opals. These composite PCs are highly desirable because the incorporation of several components with different properties may open up more possibilities for generating novel optical properties.[8−10] For example, the infiltration of gold nanoparticles (GNPs) into PCs simultaneously displays LSPR and PBG properties. However, desired inverse opals with both resonance peaks and diffraction peaks are very rare among these new composite PCs. There could be two reasons for this: first, it is not easy to uniformly infiltrate a metal into narrow interstitial regions of a colloidal crystal multilayer; and, second, the metal-

* Corresponding author. E-mail: wqian@seu.edu.cn.

(1) (a) Fujita, M.; Takahashi, S.; Tanaka, Y.; Asano, T.; Noda, S. *Science* **2005**, *308*, 1296. (b) Ogawa, S. P.; Imada, M.; Yoshimoto, S.; Okano, M.; Noda, S. *Science* **2004**, *305*, 227.

(2) (a) Sun, Y. G.; Xia, Y. N. *Science* **2002**, *298*, 2176. (b) Boyen, H. G.; Kastle, G.; Weigl, F.; Koslowski, B.; Dietrich, C.; Ziemann, P.; Spatz, J. P.; Riethmuller, S.; Hartmann, C.; Moller, M.; Schmid, G.; Garnier, M. G.; Oelhafen, P. *Science* **2002**, *297*, 1533.

(3) (a) Nath, N.; Chilkoti, A. *Anal. Chem.* **2004**, *76*, 5370. (b) Haes, A. J.; Chang, L.; Klein, W. L.; Van Duyne, R. P. *J. Am. Chem. Soc.* **2005**, *127*, 2264.

(4) (a) Yang, Y.; Hori, M.; Hayakawa, T.; Nogami, M. *Surf. Sci.* **2005**, *579*, 215. (b) Gu, Z. Z.; Horie, R.; Kubo, S.; Yamada, Y.; Fujishima, A.; Sato, O. *Angew. Chem., Int. Ed.* **2002**, *41*, 1433. (c) Wang, D. Y.; Salgueirino-Maceira, V.; Liz-Marzan, L. W.; Caruso, F. *Adv. Mater.* **2002**, *14*, 908. (d) Wang, D. Y.; Li, J. S.; Chan, C. T.; Sagueirino-Maceira, V.; Liz-Marzan, L. M.; Romanov, S.; Caruso, F. *Small* **2005**, *1*, 122.

(5) (a) Rodriguez-Gonzalez, B.; Salgueirino-Maceira, V.; Garcia-Santamaria, F.; Liz-Marzan, L. M. *Nano Lett.* **2002**, *2*, 471. (b) Romanov, S. G.; Maka, T.; Torres, C. M. S.; Muller, M.; Zentel, R. *Appl. Phys. Lett.* **1999**, *75*, 1057. (c) Romanov, S. G.; Susha, A. S.; Torres, C. M. S.; Liang, Z.; Caruso, F. *J. Appl. Phys.* **2005**, *97*, 086103.

(6) Yan, H. W.; Blanford, C. F.; Holland, B. T.; Parent, M.; Smyrl, W. H.; Stein, A. *Adv. Mater.* **1999**, *11*, 1003.

(7) Xu, X. C.; Xi, Y. G.; Han, D. H.; Liu, X. H.; Zi, J.; Zhu, Z. Q. *Appl. Phys. Lett.* **2005**, *86*, 0911121.

(8) Kuai, S. L.; Bader, G.; Ashrit, P. V. *Appl. Phys. Lett.* **2005**, *86*, 2211101.

(9) Garcia-Santamaria, F.; Salgueirino-Maceira, V.; Lopez, C.; Liz-Marzan, L. M. *Langmuir* **2002**, *18*, 4519.

(10) Fan, H. Y.; Yang, K.; Boye, D. M.; Sigmon, T.; Malloy, K. J.; Xu, H. F.; Lopez, G. P.; Brinker, C. J. *Science* **2004**, *304*, 567.

10.1021/cm060207c CCC: $33.50
Published on Web 06/30/2006

dielectric inverse opals are rather fragile and easily disrupted. Therefore, the optical properties of such metal-infiltrated PCs have been scarcely investigated.

To overcome these obstacles, considerable efforts including electrochemical metal deposition and infiltration of metal-dielectric nanoparticles have been made to prepare robust inverse opals containing metal nanoparticles. Here, we present a simple method to fabricate GNP-infiltrated polystyrene (GNIPS) inverse opal films, where individual GNPs are three-dimensionally embedded in polystyrene (PS) inverse opals. Apart from its large-scale and low-cost, the main advantages of our method are (1) stability of the immobilization of GNPs in PCs, (2) homogeneity of the distribution of individual GNPs in PCs, (3) flexibility of GNIPS films in a free-standing format, and (4) potential of GNIPS films in biological applications for immobilization of biomolecules.[11]

In this paper, we mainly investigated the optical properties of the inverse opal films with two characteristic peaks (LSPR and PBG). By varying the refractive index (RI) of the surrounding medium and the incident angle of the light, the two characteristic peaks of the GNIPS films could be freely separated and approached. This was further demonstrated by the volatilization kinetics of ethanol filling in the interstitial regions of GNIPS films. Thus, GNIPS inverse opal films may offer a new three-dimensional platform to reveal the external interactions between LSPR and PBG of those composite materials.

Experimental Section

Functionalization of Silica Sphere Surfaces with APTES. Silica spheres of ~290 nm in diameter were first purified via centrifugation and redispersion in ethanol. Next, 0.5 mL of a 98% APTES solution was added to 30 mL of a silica colloid solution of 7.2×10^{-2} g mL^{-1}. After the mixture was vigorously stirred for 6 h, APTES groups covalently bonded to the surface of silica spheres, extending their amine groups[12] outward as a new termination of silica surfaces. To remove excess reactants from the reaction mixture, the APTES-functionalized silica spheres were purified by centrifugation and redispersion in ethanol at least five times.

Preparation of Silica Colloidal Crystal Templates. Colloidal crystal templates of silica spheres[13] were fabricated on microslides by vertical deposition of APTES-functionalized silica spheres of ~290 nm in ethanol. Typically, 10 mL of an APTES-coated silica colloid solution of 2.4×10^{-2} g mL^{-1} was added to a small glass trough. Next, the microslides were mounted vertically in a silicone rubber spacer and lightly immersed into the glass trough. After alcoholic solvents volatilized spontaneously, high-quality colloidal crystal templates were obtained.

Synthesis of GNPs. By reduction of chloroauric acid with sodium borohydride, aqueous suspensions of small GNPs[14] that were ~5 nm in diameter were prepared according to literature procedures with some modifications.[15] Assuming that all chloroauric acid was reduced to ~5 nm GNPs and using the bulk density of gold, we calculated that the concentration of the obtained GNP aqueous solutions was $\sim 2 \times 10^{14}$ particles mL^{-1}.

Infiltration of GNPs into the Interstitial Regions of a Colloidal Crystal Multiplayer. Silica colloidal crystal templates were fixed into a test tube with 10 mL of a $\sim 2 \times 10^{14}$ particles mL^{-1} GNP aqueous solution. Next, the test tube was immobilized in an oscillator and kept shaking for 5 h. Thus, GNPs were adsorbed to the amine groups on silica sphere surfaces, resulting in a silica sphere covered with islands of GNPs. After that, GNP-infiltrated silica templates were rinsed with water and dried in air.

Preparation of GNIPS Inverse Opal Films. A toluene solution of PS of 0.12 g mL^{-1} (average molecular weight of 312 000) was infiltrated into the vacant spaces between the spheres. After 2−3 days, the GNIPS film together with the template was spontaneously separated from the microslide, and then the template was removed by treatment with 4% hydrofluoric acid, producing a large-area GNIPS film in a free-standing form.

Preparation of Experimental Cells. The experimental cell was assembled from two microslides, one silicone rubber spacer, and a GNIPS film. A "□" type silicone rubber spacer was mounted on the macroporous side of a GNIPS film, and then the film together with the spacer was sandwiched between two microslides. After the fabrication, the experimental cell was precisely mounted on the holder supplied by the producer. A schematic for the experimental cell is illustrated in Figure 1.

SEM and Optical Characterization. SEM characterization was carried out on a LEO 1530 VP SEM to image the morphology of the samples obtained during the entire fabrication process. All samples for SEM observation were sputtered with thin gold films. UV−vis spectra were employed to investigate the optical properties of these samples by using a Shimadzu UV3150 UV−vis spectrophotometer in a transmission mode. All transmission measurements were performed at constant regions.

Results and Discussion

A schematic outline of the procedures for producing a GNIPS inverse opal film is shown in Figure 1. First, silica spheres in ethanol were coated with 3-aminopropyltriethoxysilane (APTES) to produce a surface terminated with amine groups. These APTES-functionalized silica spheres were subsequently crystallized onto a glass slide by the vertical deposition method[16] to form a colloidal crystal template. Next, the template was immersed in an aqueous solution of GNPs. Negatively charged GNPs were infiltrated into the interstitial regions and uniformly attached on silica sphere surfaces by complexation between GNPs and amine groups. Finally, a toluene solution of PS was infiltrated into the vacant spaces between the silica spheres, and then the template was removed by treatment with hydrofluoric acid. As a result, robust GNIPS inverse opal films were formed in a free-standing form.

Figure 2A shows a typical scanning electron microscopy (SEM) image of the GNP-infiltrated silica colloidal crystal film. This indicates that the ordered structure of the silica template was maintained after the infiltration of the ~5 nm GNPs, although the GNPs adsorbed on the silica surfaces could not be detected in the field emission SEM as a result

(11) Qian, W. P.; Gu, Z. Z.; Fujishima, A.; Sato, O. *Langmuir* **2002**, *18*, 4526.
(12) Zhang, D.; Chen, Y.; Chen, H. Y.; Xia, X. H. *Anal. Bioanal. Chem.* **2004**, *379*, 1025.
(13) Jiang, P.; Bertone, J. F.; Hwang, K. S.; Colvin, V. L. *Chem. Mater.* **1999**, *11*, 2132.
(14) Tan, Y.; Ding, S. H.; Wang, Y.; Qian, W. P. *Acta Chim. Sin.* **2005**, *63*, 929.
(15) Phadtare, S.; Kumar, A.; Vinod, V. P.; Dash, C.; Palaskar, D. V.; Rao, M.; Shukla, P. G.; Sivaram, S.; Sastry, M. *Chem. Mater.* **2003**, *15*, 1944.
(16) Tan, Y.; Yang, K. J.; Cao, Y. X.; Zhou, R.; Chen, M.; Qian, W. P. *Acta Chim. Sin.* **2004**, *62*, 2089.

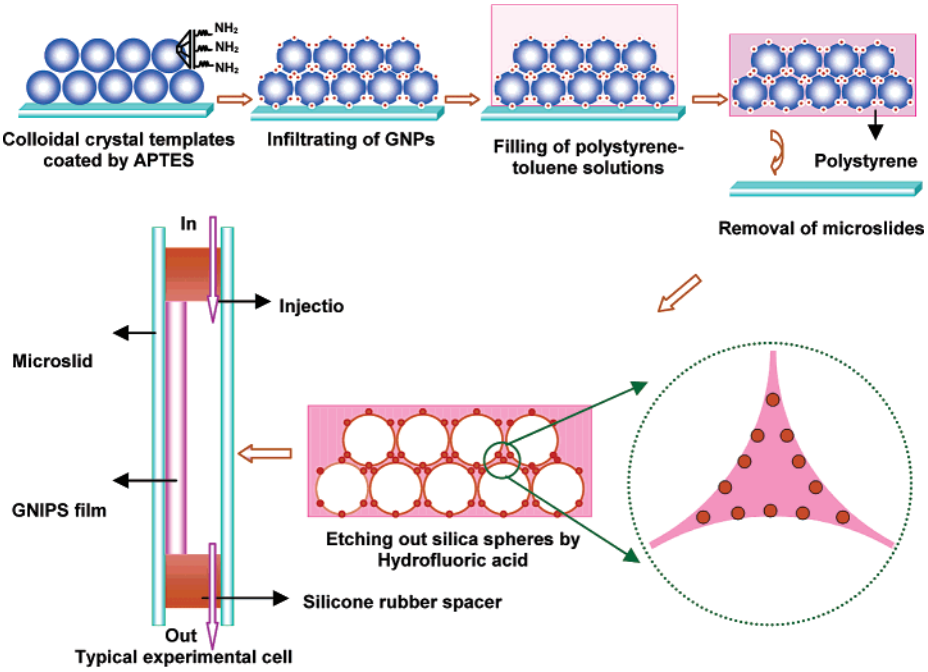

Figure 1. A schematic outline of the procedures for producing a GNIPS film and an experimental cell.

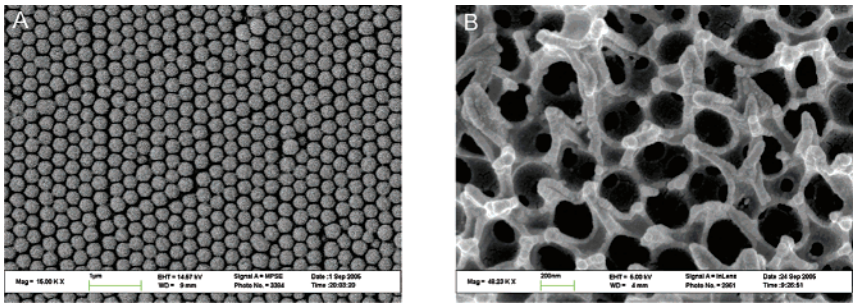

Figure 2. SEM images of (A) the GNP-infiltrated colloidal crystal template composed of ~290 nm silica spheres and (B) the cross section of the cracked GNIPS inverse opal film with ~290 nm pores.

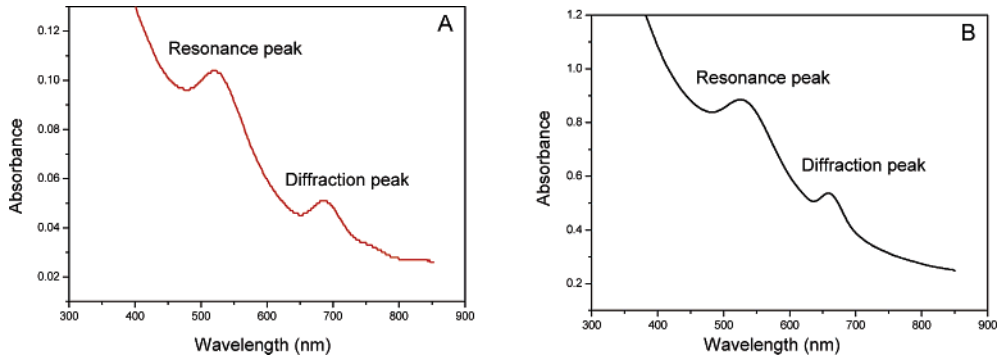

Figure 3. Absorption spectra of (A) the GNP-infiltrated silica template composed of ~290 nm silica spheres and (B) the GNIPS inverse opal film with ~290 nm pores in water.

of the resolution limit of our SEM system.[17] Figure 2B shows a SEM image of the cross section of the cracked GNIPS inverse opal film, which exhibits an ordered void structure arising from the silica spheres. It is noted that those large cavities in the film are not isolated, but rather are interconnected. Similar to Figure 2A, although the excellent ordered structure also can be observed in Figure 2B, the individual GNPs with ~5 nm cannot be found in the GNIPS film for the same reason. However, the analysis by optical absorption spectra provides an effective method for evaluating the distribution of the GNPs in GNIPS films.[18]

The quality of the samples was also assessed through UV−vis absorption spectra. Figure 3A shows a typical UV−vis spectrum of the GNP-infiltrated silica template, where the two characteristic peaks can be easily observed. The absorption peak at ~521 nm originates from the LSPR of individual GNPs. The homogeneous distribution of GNPs

(17) Miyama, T.; Yonezawa, Y. *Langmuir* **2004**, *20*, 5918.

(18) Huang, S. J.; Minami, K.; Sakaue, H.; Shingubara, S.; Takahagi, T. *J. Appl. Phys.* **2002**, *92*, 7486.

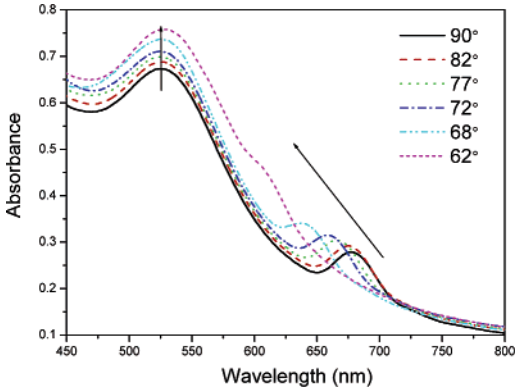

Figure 4. Absorption spectra of the GNIPS inverse opal films with ~290 nm pores in ethanol at different incident angles. The corresponding incident angles are indicated.

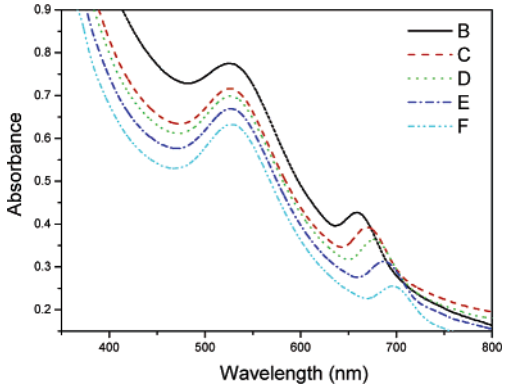

Figure 5. Absorption spectra of the GNIPS film with ~290 nm pores in media of varying RI. The media used to fill the pores are (B) water (n = 1.333), (C) 50% ethanol (V/V, ethanol−water, n = 1.346), (D) ethanol (n = 1.360), (E) 2-propanol (n = 1.377), and (F) n-butyl alcohol (n = 1.399).

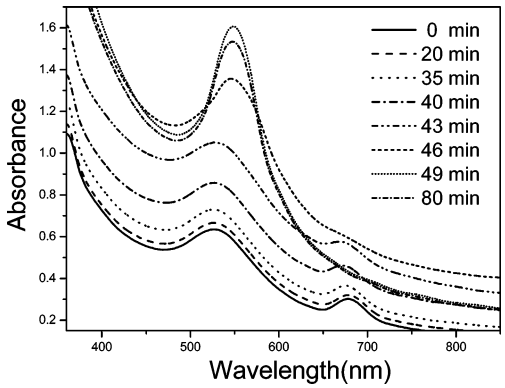

Figure 6. Evolution of the absorption spectra of the GNIPS film with ~290 nm pores during a typical volatilization of ethanol used to fill the interstitial regions. Each spectrum is labeled by the corresponding time.

in the template could be ascribed to the complexation between GNPs and amine groups, the interparticle Coulomb repulsion between adsorbed GNPs,[19] and the smaller size of the ~5 nm GNPs, allowing them to penetrate into the larger interstitial regions of the templates. The other absorption peak at ~686 nm originates from the PBG of the template consisting of the silica spheres in a face-centered-cubic lattice, which is supported by the SEM image in Figure 2A. Similar to the silica colloidal crystal template, in Figure 3B, the GNIPS inverse opal film also consists of the resonance peak and the diffraction peak, indicating that the GNIPS film replicates the photonic features of the template.

To test the stability of the immobilization of GNPs in GNIPS inverse opal films, we employed a completely closed customized flow cell (see Figure 1) to fix the GNIPS film, and then continuously rinsed the fixed film with ethanol for 3 h. The analysis by UV−vis spectra (see Supporting Information) shows no discernible difference between pre- and post-rinsing, suggesting that GNPs are stably embedded in the GNIPS film.

Initially, we investigated the evolution of the absorption spectra at different incident angles for the GNIPS inverse opal films (Figure 4). With the decrease of the incident angle from 90° to 62°, the diffraction peak is blue-shifted gradually with the increase of its intensity. The observed shifts can be attributed to the changes of the diffraction, which is related to an incident angle on the basis of Bragg diffraction equation.[20] Regarding the resonance peaks, we can see an invariance in their positions for all of the incident angles because the position of the resonance peak of GNPs does not depend on an incident angle according to Mie's theory.[21] Thus, with the decrease of the incident angle, the diffraction peak gradually approaches the resonance peak and shifts to shorter wavelength. Hence, we can expect to effectively control the approach and separation of LSPR and PBG in composite PCs by varying the incident angle.

Because of the dependences of both LSPR and PBG on the refractive index (RI) of the surrounding media, we investigated the influences of the media of varying RI upon the spectrum of the GNIPS film. Figure 5 shows that with the increase of the RI from 1.333 to 1.399, the diffraction peak is red-shifted from 659 to 696 nm, which can be explained by the variation of the effective RI of the GNIPS film. In contrast, the resonance peaks remain at approximately the same wavelength, because the GNPs may be mostly embedded in the GNIPS film so that they are not sufficiently sensitive to the change of the RI of the filling media. Thus, it is demonstrated that the GNIPS film can be used to control the shifts of the PBG by filling the macroporous samples with various media, and to "fix" the LSPR by sufficiently embedding the GNPs in GNIPS films.

We also obtained a sequence of absorption spectra during a typical volatilization of ethanol in the interstitial regions of the GNIPS film. The spectra recorded from 360 to 850 nm every few minutes are illustrated in Figure 6. At time t = 0 min, there are two obvious characteristic peaks in the spectrum of the GNIPS film. As the evolution proceeds, the resonance peak is gently red-shifted, while the diffraction peak is gradually blue-shifted with the increase of its intensity. Moreover, the diffraction peak gets closer and closer to the resonance peak, so as to induce a significant interaction between the two peaks. At time t = 46 min, the diffraction peak almost disappears. As a result, the two characteristic peaks gradually change into one.

As compared to the resonance peak, the diffraction peak undergoes an obvious shift from 679 to 547 nm during the volatilization of ethanol. Within 14 min from 35 to 49 min,

(19) Pham, T.; Jackson, J. B.; Halas, N. J.; Lee, T. R. *Langmuir* **2002**, *18*, 4915.
(20) Gu, Z. Z.; Hayami, S.; Kubo, S.; Meng, Q. B.; Einaga, Y.; Tryk, D. A.; Fujishima, A.; Sato, O. *J. Am. Chem. Soc.* **2001**, *123*, 175.
(21) Averitt, R. D.; Sarkar, D.; Halas, N. J. *Phys. Rev. Lett.* **1997**, *78*, 4217.

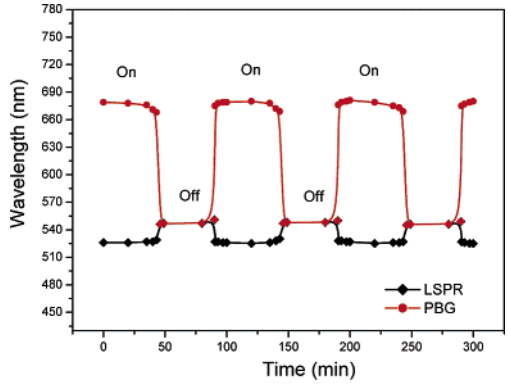

Figure 7. Effect of the volatilization and permeation of ethanol on the positions of the resonance peaks (◆) and the diffraction peaks (●).

the diffraction peak is blue-shifted by ~9.2 nm per unit time, while the resonance peak is red-shifted by ~1.4 nm per unit time. The result suggests that the volatilization of ethanol has an opposite effect on the shifts of the diffraction peak and the resonance peak. The resonance peak in Figure 6 undergoes an obvious red-shift during the volatilization of ethanol. This phenomenon could be attributed to a gradually stronger scattering, because the contrast between the PS inverse opal and its voids is gradually larger than the precursors.[9] In the final stage of the ethanol volatilization, only one characteristic peak can be observed in the absorption spectra, suggesting that the diffraction peak could be incorporated with the resonance peak.

Figure 7 illustrates the changes of the two characteristic peaks during the repeated processes of ethanol volatilizing and permeating. In each cycle, the diffraction peak first approaches gradually with the resonance peak due to the slow volatilization of ethanol. Next, the diffraction peak rapidly separates from the resonance peak due to the fast permeation of ethanol. As the cycle of volatilization and permeation proceeds, the two characteristic peaks of the GNIPS film exhibit a reversible shift. As shown in Figure 7, an interesting feature of the GNIPS film is its ability to optically "switch on−off" in response to the changes of embedded solvents. This suggests that the feature of the GNIPS films may be useful for monitoring the environmental changes by the permeation and release of surrounding media. In addition, the GNIPS films could be also used to quantitatively analyze the volatile solvents at different concentrations according to the differences of the periodicity of volatilizing and filling.[22]

Conclusion

In conclusion, we have demonstrated a simple route for preparing high-quality GNIPS inverse opal films, which combine the LSPR properties of individual GNPs and the PBG features of silica colloidal crystal templates. These GNIPS films are attractive because, by altering the incident angle and the RI of the permeated media, we can effectively control the separation and approach of LSPR and PBG over a wide wavelength range. In addition, we have illustrated the volatilization kinetics of ethanol filling in the interstitial regions of the GNIPS films to reveal the possible interactions between LSPR and PBG in composite PCs. The incorporation of GNPs and PCs may provide a new opportunity to manipulate the combined optical signals, which may have potential applications such as in environmental monitoring, vapor-sensing, and bio-catalyzing.

Acknowledgment. This research is supported by the National Nature Science Foundation of China (Nos. 20475009, 30370312), the Foundation for the Author of National Excellent Doctoral Dissertation of PR China (No. 200252), and the Foundation for Excellent Doctoral Dissertation of Southeast University.

Supporting Information Available: Additional figures and text. This material is available free of charge via the Internet at http://pubs.acs.org.

CM060207C

(22) Vossmeyer, T.; Guse, B.; Besnard, I.; Bauer, R. E.; Müllen, K.; Yasuda, A. *Adv. Mater.* **2002**, *14*, 238.